Asian Journal of Chemistry; Vol. 34, No. 4 (2022), 1021-1026

ASIAN JOURNAL OF CHEMISTRY

https://doi.org/10.14233/ajchem.2022.23730

An Experimental Analysis of Silk Cocoon Layer-PANI Polymer Composite as Electrode for Thermoelectric Generator Application

SINDHU SREE MURALIDHAR[1], NAVYARANI MARLINGAIAH[2], VINAY GANGARAJU[1], MAHESH SHASTRI[1,3], MURTHY MUNIYAPPA[1,3], SUSHIL KUMAR SINGH[4], PRASANNA D. SHIVARAMU[1], ANANDA KUMAR C S[1] and DINESH RANGAPPA[1,*]

[1]Department of Applied Sciences (Nanotechnology), Centre for Post-Graduation Studies, Visvesvaraya Technological University, Muddenahalli Campus, Chikkaballapura-562101, India
[2]Department of Applied Sciences, Dayanand Sagar University, Kumar Swamy Layout, Bengaluru-560111, India
[3]Department of Electronics & Communication, Nagarjuna College of Engineering & Technology, Devanahalli, Bengaluru-562164, India
[4]Functional Materials Group, Solid State Physics Laboratory, Defence Research Development Organization, New Delhi-110054, India

*Corresponding author: E-mail: dineshrangappa@gmail.com; dinesh.rangappa@vtu.ac.in

Received: 17 January 2022; *Accepted*: 28 February 2022; *Published online*: 10 March 2022; AJC-20749

In this study, a silk cocoon layer (SCL) was surface coated with polyaniline (PANI), which serves as an electrode for thermoelectric generator (TEG) application. Here, the PANI was synthesized using the sol-gel method and coated on both sides of SCL using doctor-blade method. The efficiency of converting thermal energy into electrical energy was analyzed with a temperature range from 30 to 60 ºC. The TG-DTA analysis was performed to evaluate thermal stability. An evident change in the resistance was noticed for both cold (~5 °C) and heat (60 ºC) respective temperatures. Thus, this study provides a new biomaterial-based TEG electrode for waste heat recovery system/thermal management.

Keywords: Silk cocoon, Polyaniline, Thermoelectric generator, Polymer nanocomposite.

INTRODUCTION

With the depletion of fossil fuels, interest in renewable energy is increasing significantly [1,2]. Electrical energy can be harvested from renewable sources such as heat, mechanical force, light, *etc*. Among many renewable energy technologies thermal electric generator (TEG) is one of the interesting renewable energy sources [3]. In TEGs electric potential and heat are seamlessly converted in to electrical energy. These TEGs are categorized into two types namely, the Seebeck effect and the Peltier effect. In Seebeck effect, the electric potential is generated based on the difference in temperature applied between two different metals. The Peltier effect which is the exact opposite of Seebeck effect, which controls heat generation by applied electric potential [4-7]. These TEGs have the great advantage of operating at different temperatures, environmentally friendly, no movable mechanical parts, low cost and easy maintenance [5,8,9]. Conventional inorganic semiconductors such as SnSe, Cu_2Se, $CoSb_3$, SiGe, Bi_2Te_3 and PbTe have been reported as electrode material for many thermal devices due to their excellent thermoelectric properties. However, the difficulty in synthesis and high cost has restricted their application in thermoelectric devices [10-12]. In addition, the existing TEGs are too bulky and rigid. Therefore, over the past decades an intense research has been going on for developing sustainable and eco-friendly materials using flexible and biomaterial based thermoelectric devices. Such biomaterials based TEG have a potential interest in the field of electronic devices for environment, health and safety applications [13-15].

Alternatively polymer materials have been attracted the most due to their lightweight, easy processing and mechanical stability [16,17]. The most commonly preferred thermoelectric polymer materials are polypyrrole [18], polyacetylene [19], polythiophene [20], polyethylene dioxythiophene [21-24], poly(3-hexylthiophene) [25,26] and polyaniline (PANI) [27-29]. However, these materials have poor resistance and unsuitable for high temperatures applications. Further these polymer materials have low thermal conductivity than those of inorganic material. Hence to use polymer for TEG application, the materials which operate at low temperature (< 100 ºC) are required [30-32].

Among many natural polymer materials, there has been increased interest inclined towards silk cocoon biomaterial because of its natural abundance and eco-friendly nature. Silk cocoon also offers excellent mechanical, thermal, adhesive and biocompatible properties suitable for different applications [14,33-39]. Silk cocoon has a complex nanostructure with dimensions of several to hundreds of nanometers. It consists of β sheet structure which is made up of nanofibril bundles and nanocrystals with 20-80 nm in diameter [39]. These structures enable the integration of strength, stiffness and toughness in natural silk fibers [40-43]. However, silk is a poor conductor of electricity, but susceptible to static electrical charge [44].

Several researchers have reported thermal properties of silk fibers [45-49]. Xue *et al*. [42-46] reported that the thermal conductivity, θ value, of silk fiber in the axial direction is ranges from 0.54-6.53 W/mK. However, when silk fibers were stretched, the θ value was up to 13.1 W/mK. The silk films produce low thermal conductivity in the cross-plane direction. Similarly, Zhou *et al*. [50] have reported the electrical and thermal properties of S-shaped silk fabric coated with MWCNT. In an infrared image, they have noticed that with an increase in temperature and voltage the image will become brighter and brighter. This shows that the fiber coated with conducting material is influenced by the heat. There is potential interest in coating conductive polymer with silk cocoon layers to improve the thermal conductivity, as there are not many reports on exploiting conductive polymer PANI for this purpose.

In this work, a silk cocoon layer (SCL) surface coated with polyaniline (PANI) as an electrode for polymer-based thermoelectric generators is reported. Based on our findings, it is demonstrated that the silk cocoon composited with PANI can be used to exploit the heat energy in to electrical energy.

EXPERIMENTAL

Silk cocoon were procured from a central silk board (Bengaluru, India). The chemicals *viz*. aniline, hydrochloride acid and ammonium persulfate were purchased and used for polyaniline (PANI) synthesis. All chemicals were of analytical grade and used directly without further purification in this work.

Preparation of SCL-PANI: Polyaniline (PANI) was synthesized using sol-gel method. Here, a 20 mL of aniline was added to 250 mL of aqueous HCl and stirred under an ice bath for 30 min. To this aqueous solution, ammonium persulfate was added dropwise until the formation of gelation. This suspension was further stirred for 1 h. For purification, this suspension was washed with methanol and distilled water. The solution was subjected to dry for 48 h under 90 ºC in a vacuum. A silk cocoon layer (SCL) was dissected to 1 cm × 1 cm from a silk cocoon. PANI (2 mg) was grinded for 2 min in distilled water as a medium in mortal and pestle. This suspension was coated on SCL using the doctor blade method and dried overnight at room temperature.

Characterization: The surface morphology and elemental analysis of SCL, PANI and SCL-PANI samples were observed by scanning electron microscopy (SEM, Hitachi SU1510) and EDAX (Thermo-Fisher Scientific) equipped after coating with gold. X-ray diffraction XRD (Rigaku IV) analysis of samples was performed using Cu*K*α1 radiation operated at 35 kV and 25 mA from 10º to 80º with a step width of 0.02. The functional group analysis was performed using Fourier transform infrared spectroscopy (Perkin-Elmer STA8000) at 4000-400 cm^{-1}. An electrochemical workstation (Keithley 2400 SMU model) was employed.

RESULTS AND DISCUSSION

Crystal structure analysis of SCL and SCL/PANI: The XRD in Fig. 1 show crystal structure of SCL and SCL-PANI polymer composite. It is observed that the diffraction peak at 2θ = 20.6º represents the silk-IIβ pleated sheet [51-54], whereas 2θ = 14.48º, is the quantum transfer of PANI with a length of the conjugate π-π bond and diffraction peak at 25.53º indicates the polymer chain of the PANI [55]. When the PANI is deposited on the cocoon layer the intensity characteristics of PANI are reduced, which indicates the formation of composite between the side-chain protein structure of the fiber and PANI. After coating PANI on the fibers, there is no significant change noticed in the β-pleated sheet. This is considerable due to the fact that the thermal stability of the fiber depends on the presence of β pleated sheets [45]. Hence, from the XRD patterns, it is evident that the presence of β pleated sheets of the fiber after composition with PANI shows stability of the material towards temperature.

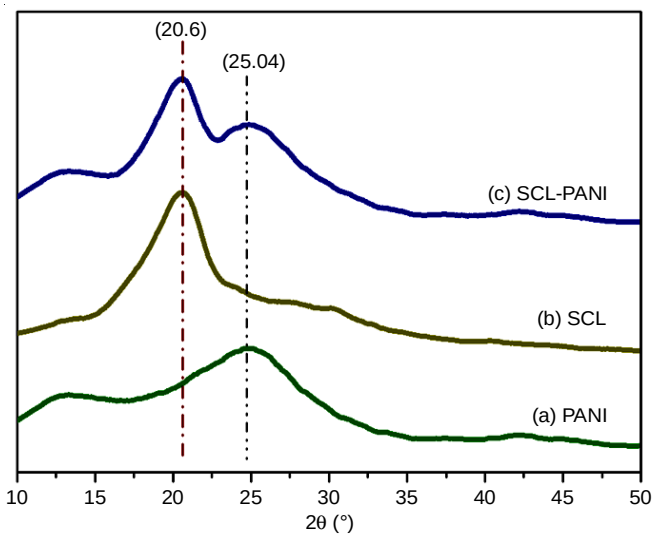

Fig. 1. X-Ray diffractometer spectra of (a) PANI, (b) silk cocoon layer and (c) silk cocoon layer-PANI

Morphology analysis of SCL and SCL/PANI: In order to verify the surface morphology of SCL-PANI, PANI and SCL were characterized using SEM images are shown in Fig. 2. It is noticeable that the surface of silk fibers is lustrous, smooth in texture. From Fig. 2c-d, it is also observed that the small particles spotted on the fibers is sericin (glue-like) protein [52]. The PANI particles synthesized using the sol-gel method is shown in Fig. 2a-b. The result indicates agglomerated particles with stacked layers formation. After the surface coating of PANI on the fiber layer results in a change on the surface of the fiber

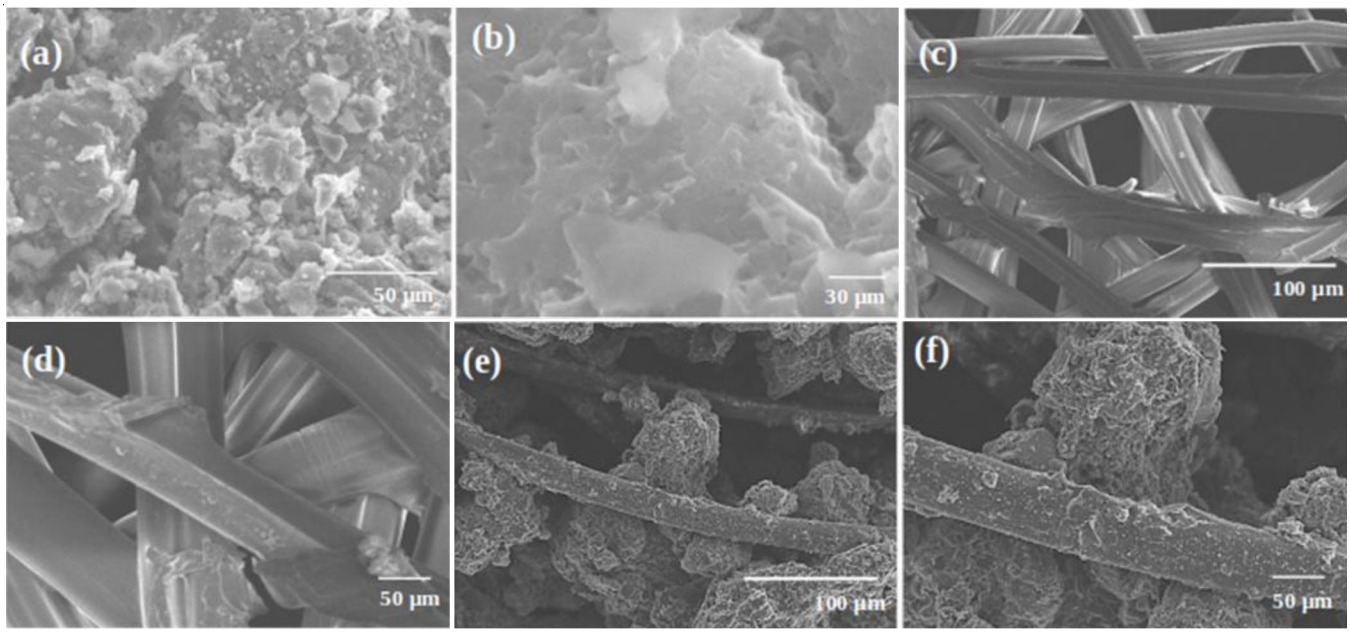

Fig. 2. SEM images of PANI particles (a-b), bare silk cocoon layer (c-d) and silk cocoon layer-PANI polymer composite (e-f)

(Fig. 2e-f). The fibers have swollen and PANI particles are being deposited on the surface of the fiber. This indicates the formation of SCL-PANI polymer composite. Hence, the uniform distribution of PANI on the surface of the fiber refers to the continuous conductivity with the influence of heat. However, due to rigidity, a strong bond interaction chain of the PANI is poor. This resulted in some large particles coating on the surface of the composite fiber.

Functional group analysis of SCL and SCL-PANI: The chemical bond analysis of SCL and SC-PANI was further analyzed using Fourier-transform infrared spectroscopy (FT-IR) in the range from 4000 to 400 cm^{-1} as shown in Fig. 3. The spectral bands at 1227.24, 1617.88, 1514.47 and 1137.17 cm^{-1} refers to amide I, II and III, respectively which are attributed to the secondary structure of silk α-helix and β-pleated sheet [16,27,28]. Hence no significant difference was noticed in the fingerprint region of SCL after coating PANI and this result corresponds to the XRD spectra where the β-sheets are not affected. However, at 2892.2 cm^{-1} and 2965.5 cm^{-1}, there was a decrease in the intensity of the peak in SCL-PANI. This spectral range refers to the carboxyl group (C-OH), indicating that carbon particles have interacted with the backbone hydrogen chain of protein structure. Due to the interaction of polymer chain there, there is a good thermal stability and it is uniformly deposited.

The TG-DTA is used to analyze the thermal stability of SCL and SCL-PANI polymer composite and results are presented in Fig. 4. The weight loss in cocoon layer started at 150 ºC indicating the loss of water content by evaporation. Further with increased temperature, there is fast decomposition of SCL was observed as it turned black ash around 400 ºC. In the SCL-PANI polymer composite, the weight loss was started around 300 ºC, which is due to carbon chains of PANI. Hence, the result shows the increase in the fiber's thermal stability of with the composition of PANI. Further an increase in the weight was measured by the following equation [56]:

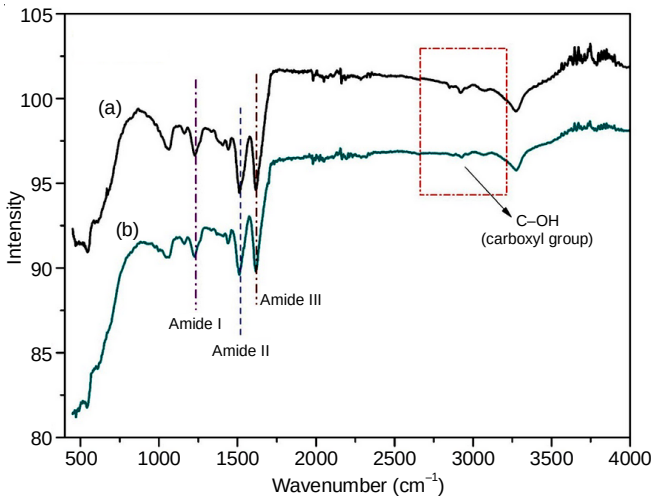

Fig. 3. FTIR spectra of (a) silk cocoon layer-PANI and (b) silk cocoon layer

$$\omega = \frac{m_2 - m_1}{m_1} \times 100\%$$

The ω is the percent of weight increased, m_2 is the weight of SCL-PANI composite and m_1 is the weight of SCL. The result shows 48.64% total retained weight of the sample.

Electrical measurements of SCL and SCL-PANI: The current and voltage characteristics of silk cocoon layer and SCL-PANI samples were measured varying the temperatures. The electrical measurements were carried out in a potential window between -10 V to 10 V. Fig. 5 shows the I-V characteristics of SCL and SCL-PANI in the temperature range from 30 to 60 ºC. Under the influence of temperature, bare SCL shows negligible small current due to its high resistance as it is insulating nature. The current produced by SCL is few microamps and hence it is not considered. Similarly, the SCL-PANI polymer composite shows current generation upto 0.04 A for the above specified temperature range. Thus, it is clearly evident

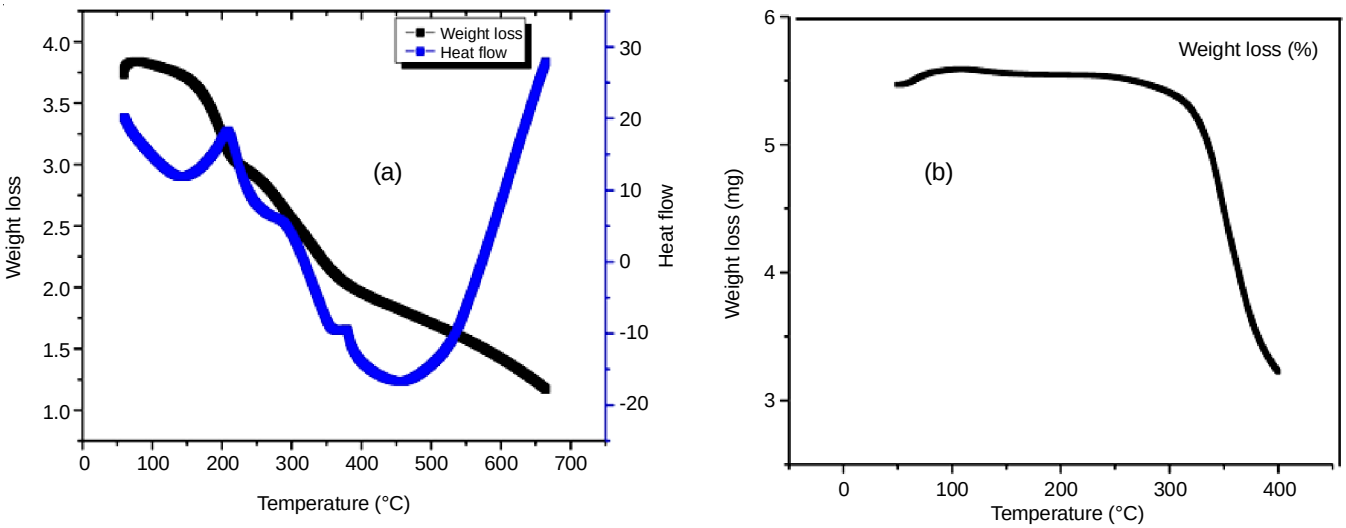

Fig. 4. TG-DTA analysis of SCL (a) and SCL-PANI (b) polymer composite measured under N_2 gas environment

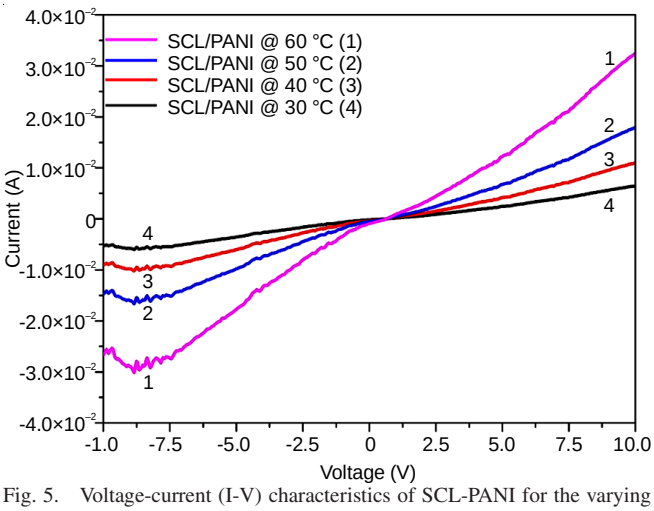

Fig. 5. Voltage-current (I-V) characteristics of SCL-PANI for the varying temperature from 30 to 60 ºC

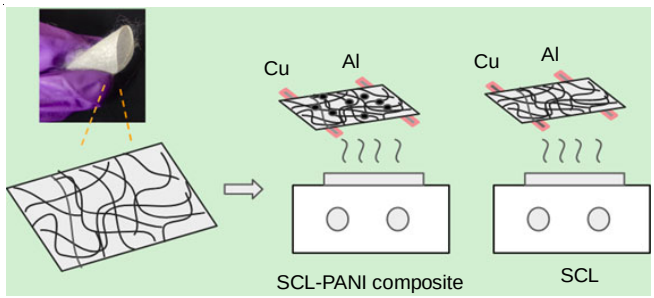

Fig. 6. Schematic of thermal analysis for both SCL and SCL-PANI polymer composites

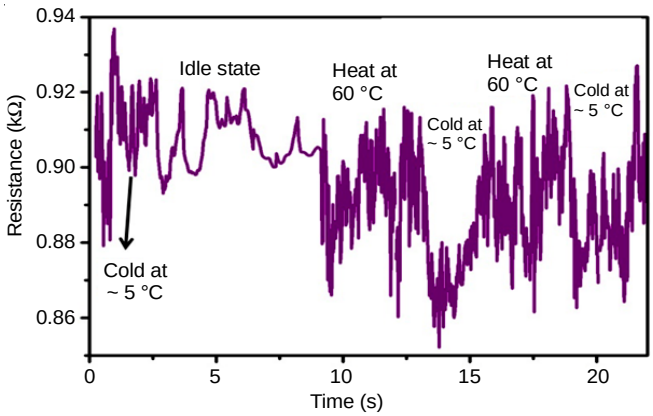

Fig. 7. Resistance measurement of SCL-PANI under cold and heat temperature. The results were considered with the varying in resistance with respect to time

that the naturally SCL has thermal conductivity, it is further increased with the coating of PANI, by providing a conductive medium along the fiber. This also shows the well adhesive of PANI with silk fibers helps in promoting the current flow in the network.

Performance of SC-PANI based thermoelectric generator (TEG): Fig. 6 shows the schematic setup for the thermal analysis for the generation of temperature difference. The SCL has coated both sides with PANI and hence stitched with copper sheets for the electrical contact. Since, we are using the Seebeck coefficient method, the voltage is generated with respect to the heat applied to the different metals. Here, the aluminum sheet is used as counter electrode and copper connected SCL-PANI as a working electrode. It was found that there is a linear increase in the voltage with respect to the temperature applied (Fig. 6). Further, the electrodes were subjected to different temperature from ~5 ºC (cold) to 60 ºC (hot) and noted down its change in resistance with respect to time (Fig. 7). It is observed that there is decrease in resistance in cold and *vice-versa* in hot. Thus, this finding clearly shows that the SCL-PANI synthesized *via* simple route can be used as thermal electrodes.

Conclusion

In summary, a bio-TEG electrode was developed using a silk cocoon layer coated with PANI for harvesting electrical energy from waste heat. The PANI was synthesized using sol-gel method. XRD, SEM, FTIR, TGA and I-V were used to characterized SCL-PANI as thermal electrode. The thermal property of SCL without and with coated PANI was analyzed and found there is an increase in the thermal stability of SCL coated with PANI sample. All studies were carried out for the

thermal range between 30 to 60 ºC. In addition an evident change in the resistance was noticed for both cold (~5 ºC) and heat (60 ºC) temperatures. Based on present findings, it is proposed that this new approach would be used as electrodes for wearable electronics, e-textiles, waste heat management, energy harvesting and thermal sensor.

CONFLICT OF INTEREST

The authors declare that there is no conflict of interests regarding the publication of this article.

REFERENCES

1. G. Zhu, R. Yang, S. Wang and Z.L. Wang, *Nano Lett.*, **10**, 3151 (2010); https://doi.org/10.1021/nl101973h
   K.-I. Park, M. Lee, Y. Liu, S. Moon, G.-T. Hwang, G. Zhu, J.E. Kim, S.O. Kim, D.K. Kim, Z.L. Wang and K.J. Lee, *Adv. Mater.*, **24**, 2999 (2012); https://doi.org/10.1002/adma.201200105
2. C. Chang, V.H. Tran, J. Wang, Y.K. Fuh and L. Lin, *Nano Lett.*, **10**, 726 (2010); https://doi.org/10.1021/nl9040719
3. F.-R. Fan, Z.-Q. Tian and Z. Lin Wang, *Nano Energy*, **1**, 328 (2012); https://doi.org/10.1016/j.nanoen.2012.01.004
4. P.M. Kumar, V. Jagadeesh Babu, A. Subramanian, A. Bandla, N. Thakor, S. Ramakrishna and H. Wei, *Designs*, **3**, 22 (2019); https://doi.org/10.3390/designs3020022
5. Z.B. Tang, Y.D. Deng, C.Q. Su, W.W. Shuai and C.J. Xie, *Case Stud. Therm. Eng.*, **5**, 143 (2015); https://doi.org/10.1016/j.csite.2015.03.006
6. K.K. Jung, Y. Jung, C.J. Choi, J.M. Lee and J.S. Ko, *Curr. Appl. Phys.*, **16**, 1442 (2016); https://doi.org/10.1016/j.cap.2016.08.010
7. C. Gould, N. Shammas, S. Grainger and I. Taylor, A Comprehensive Review of Thermoelectric Technology, Microelectrical, and Power Generation Properties; In Proceedings of the 26th International Conference on Microelectronics, Nis, Serbia & Montenegro, pp. 329-332, 11–14 May (2008).
8. A. Shakouri, *Annu. Rev. Mater. Res.*, **41**, 399 (2011); https://doi.org/10.1146/annurev-matsci-062910-100445
9. R. Ahiska and S. Dislitas, *Energy Convers. Manage.*, **52**, 27 (2011); https://doi.org/10.1016/j.enconman.2010.06.023
10. R. Kroon, D.A. Mengistie, D. Kiefer, J. Hynynen, J.D. Ryan, L. Yu and C. Müller, *Chem. Soc. Rev.*, **45**, 6147 (2016); https://doi.org/10.1039/C6CS00149A
11. Y. Chen, Y. Zhao and Z. Liang, *Energy Environ. Sci.*, **8**, 401 (2015); https://doi.org/10.1039/C4EE03297G
12. Y. Du, S.Z. Shen, K. Cai and P.S. Casey, *Prog. Polym. Sci.*, **37**, 820 (2012); https://doi.org/10.1016/j.progpolymsci.2011.11.003
13. G.H. Altman, F. Diaz, C. Jakuba, T. Calabro, R.L. Horan, J.S. Chen, H. Lu, J. Richmond and D.L. Kaplan, *Biomaterials*, **24**, 401 (2003); https://doi.org/10.1016/S0142-9612(02)00353-8
14. B.M. Min, G. Lee, S.H. Kim, Y.S. Nam, T.S. Lee and W.H. Park, *Biomaterials*, **25**, 1289 (2004); https://doi.org/10.1016/j.biomaterials.2003.08.045
15. B. Saravanakumar, R. Mohan, K. Thiyagarajan and S.J. Kim, *RSC Adv.*, **3**, 16646 (2013); https://doi.org/10.1039/c3ra40447a
16. B. Russ, A. Glaudell, J.J. Urban, M.L. Chabinyc and R.A. Segalman, *Nat. Rev. Mater.*, **1**, 16050 (2016); https://doi.org/10.1038/natrevmats.2016.50
17. M. He, F. Qiu and Z. Lin, *Energy Environ. Sci.*, **6**, 1352 (2013); https://doi.org/10.1039/c3ee24193a
18. H. Kaneko, T. Ishiguro, A. Takahashi and J. Tsukamoto, *Synth. Met.*, **57**, 4900 (1993); https://doi.org/10.1016/0379-6779(93)90836-L
19. N.T. Kemp, A.B. Kaiser, C.J. Liu, B. Chapman, O. Mercier, A.M. Carr, H.J. Trodahl, R.G. Buckley, A.C. Partridge, J.Y. Lee, C.Y. Kim, A. Bartl, L. Dunsch, W.T. Smith and J.S. Shapiro, *J. Polym. Sci., B, Polym. Phys.*, **37**, 953 (1999); https://doi.org/10.1002/(SICI)1099-0488(19990501)37:9<953::AID-POLB7>3.0.CO;2-L
20. B.Y. Lu, C.C. Liu, S. Lu, J.K. Xu, F.X. Jiang, Y.Z. Li and Z. Zhang, *Chin. Phys. Lett.*, **27**, 057201 (2010); https://doi.org/10.1088/0256-307X/27/5/057201
21. O. Bubnova, Z.U. Khan, H. Wang, S. Braun, D.R. Evans, M. Fabretto, P. Hojati-Talemi, D. Dagnelund, J.-B. Arlin, Y.H. Geerts, S. Desbief, D.W. Breiby, J.W. Andreasen, R. Lazzaroni, W.M. Chen, I. Zozoulenko, M. Fahlman, P.J. Murphy, M. Berggren and X. Crispin, *Nat. Mater.*, **13**, 190 (2014); https://doi.org/10.1038/nmat3824
22. G.H. Kim, L. Shao, K. Zhang and K.P. Pipe, *Nat. Mater.*, **12**, 719 (2013); https://doi.org/10.1038/nmat3635
23. O. Bubnova, M. Berggren and X. Crispin, *J. Am. Chem. Soc.*, **134**, 16456 (2012); https://doi.org/10.1021/ja305188r
24. O. Bubnova, Z.U. Khan, A. Malti, S. Braun, M. Fahlman, M. Berggren and X. Crispin, *Nat. Mater.*, **10**, 429 (2011); https://doi.org/10.1038/nmat3012
25. S.Y. Qu, Q. Yao, L.M. Wang, Z.H. Chen, K.Q. Xu, H.R. Zeng, W. Shi, T. Zhang, C. Uher and L. Chen, *NPG Asia Mater.*, **8**, e292 (2016); https://doi.org/10.1038/am.2016.97
26. Q. Zhang, Y.M. Sun, W. Xu and D.B. Zhu, *Energy Environ. Sci.*, **5**, 9639 (2012); https://doi.org/10.1039/c2ee23006b
27. L.M. Wang, Q. Yao, J.X. Xiao, K.Y. Zeng, W. Shi, S.Y. Qu and L. Chen, *Chem. Asian J.*, **11**, 1955 (2016); https://doi.org/10.1002/asia.201600493
28. Q. Yao, Q. Wang, L. Wang, Y. Wang, J. Sun, H. Zeng, Z. Jin, X. Huang and L. Chen, *J. Mater. Chem. A Mater. Energy Sustain.*, **2**, 2634 (2014); https://doi.org/10.1039/C3TA14008C
29. H. Wang, L. Yin, X. Pu and C. Yu, *Polymer*, **54**, 1136 (2013); https://doi.org/10.1016/j.polymer.2012.12.038
30. M.A. Kamarudin, S.R. Sahamir, R.S. Datta, B.D. Long, M.F. Mohd Sabri and S. Mohd Said, *Scient. World J.*, **2013**, 713640 (2013); https://doi.org/10.1155/2013/713640
31. Y. Sun, P. Sheng, C. Di, F. Jiao, W. Xu, D. Qiu and D. Zhu, *Adv. Mater.*, **24**, 932 (2012); https://doi.org/10.1002/adma.201104305
32. R. Yue, S. Chen, C. Liu, B. Lu, J. Xu, J. Wang and G. Liu, *J. Solid State Electrochem.*, **16**, 117 (2012); https://doi.org/10.1007/s10008-011-1292-0
33. M. Lee, Y.G. Ko, J.B. Lee, W.H. Park, D. Cho and O.H. Kwon, *Macromol. Res.*, **22**, 746 (2014); https://doi.org/10.1007/s13233-014-2096-8
34. D.N. Rockwood, R.C. Preda, T. Yucel, X.Q. Wang, M.L. Lovett and D.L. Kaplan, *Nat. Protoc.*, **6**, 1612 (2011); https://doi.org/10.1038/nprot.2011.379
35. J. Perez-Rigueiro, C. Viney, J. Llorca and M. Elices, *J. Appl. Polym. Sci.*, **75**, 1270 (2000); https://doi.org/10.1002/(SICI)1097-4628(20000307)75:10<1270::AID-APP8>3.0.CO;2-C
36. G.Y. Liu, Q. Tang, Y.N. Yu, J. Li, J.W. Luo and M.Z. Li, *Polym. Adv. Technol.*, **25**, 1596 (2014); https://doi.org/10.1002/pat.3408
37. B.M. Min, L. Jeong, K.Y. Lee and W.H. Park, *Macromol. Biosci.*, **6**, 285 (2006); https://doi.org/10.1002/mabi.200500246
38. F. Zhang, B.Q. Zuo and L. Bai, *J. Mater. Sci.*, **44**, 5682 (2009); https://doi.org/10.1007/s10853-009-3800-5
39. S. Ling, D.L. Kaplan and M.J. Buehler, *Nat. Rev. Mater.*, **3**, 18016 (2018); https://doi.org/10.1038/natrevmats.2018.16
40. Y. Wang, J. Guo, L. Zhou, C. Ye, F.G. Omenetto, D.L. Kaplan and S. Ling, *Adv. Funct. Mater.*, **28**, 1805305 (2018); https://doi.org/10.1002/adfm.201805305
41. S. Ling, W. Chen, Y. Fan, K. Zheng, K. Jin, H. Yu, M.J. Buehler and D.L. Kaplan, *Prog. Polym. Sci.*, **85**, 1 (2018); https://doi.org/10.1016/j.progpolymsci.2018.06.004

42. J.L. Yarger, B.R. Cherry and A. van der Vaart, *Nat. Rev. Mater.*, **3**, 18008 (2018); https://doi.org/10.1038/natrevmats.2018.8
43. R. Xiong, A.M. Grant, R. Ma, S. Zhang and V.V. Tsukruk, *Mater. Sci. Eng.*, **125**, 1 (2018); https://doi.org/10.1016/j.mser.2018.01.002
44. H.-J. Kim, J.-H. Kim, K.-W. Jun, J.-H. Kim, W.-C. Seung, O.H. Kwon, J.-Y. Park, S.-W. Kim and I.-K. Oh, *Adv. Energy Mater.*, **6**, 1502329 (2016); https://doi.org/10.1002/aenm.201502329
45. Y. Xue, S. Lofland and X. Hu, *Polymers*, **11**, 456 (2019); https://doi.org/10.3390/polym11030456
46. X. Jin, J. Zhang, W. Gao, J. Li and X. Wang, *Biointerphases*, **9**, 031013 (2014); https://doi.org/10.1116/1.4890982
47. J. Zhang, R. Rajkhowa, J. Li, X. Liu and X. Wang, *Mater. Des.*, **49**, 842 (2013); https://doi.org/10.1016/j.matdes.2013.02.006
48. S. Xu, Z. Xu, J. Starrett, C. Hayashi and X. Wang, *Polymer*, **55**, 1845 (2014); https://doi.org/10.1016/j.polymer.2014.02.020
49. A. Delan, M. Rennau, S.E. Schulz and T. Gessner, *Microelectron. Eng.*, **70**, 280 (2003); https://doi.org/10.1016/S0167-9317(03)00417-9
50. J. Zhou, Z. Zhao, R. Hu, J. Yang, H. Xiao, Y. Liu and M. Lu, *Mater. Des.*, **191**, 108636 (2020); https://doi.org/10.1016/j.matdes.2020.108636
51. J.-T. Wang, L.-L. Li, M.-Y. Zhang, S.-L. Liu, L.-H. Jiang and Q. Shen, *Mater. Sci. Eng. C*, **34**, 417 (2014); https://doi.org/10.1016/j.msec.2013.09.041
52. J.-T. Wang, L.-L. Li, L. Feng, J.-F. Li, L.-H. Jiang and Q. Shen, *Int. J. Biol. Macromol.*, **63**, 205 (2014); https://doi.org/10.1016/j.ijbiomac.2013.11.006
53. K.I. Lee, X. Wang, X. Guo, K.-F. Yung and B. Fei, *Int. J. Biol. Macromol.*, **95**, 826 (2017); https://doi.org/10.1016/j.ijbiomac.2016.11.090
54. B. Gupta, N. Kumar, K. Panda, V. Kanan, S. Joshi and I. Visoly-Fisher, *Sci. Rep.*, **7**, 45030 (2017); https://doi.org/10.1038/srep45030
55. S. Ambalagi, M. Devendrappa, S. Nagaraja and B. Sannakki, *IOP Conf. Series Mater. Sci. Eng.*, **310**, 012081 (2018); https://doi.org/10.1088/1757-899X/310/1/012081
56. Z. Ma, W. Wang and D. Yu, *J. Mater. Sci.*, **55**, 796 (2020); https://doi.org/10.1007/s10853-019-04035-0